frontiers in Microbiology

ORIGINAL RESEARCH
published: 04 December 2018
doi: 10.3389/fmicb.2018.02947

A Genome-Scale Metabolic Model for *Methylococcus capsulatus* (Bath) Suggests Reduced Efficiency Electron Transfer to the Particulate Methane Monooxygenase

Christian Lieven[1], Leander A. H. Petersen[2,3], Sten Bay Jørgensen[3], Krist V. Gernaey[3], Markus J. Herrgard[1] and Nikolaus Sonnenschein[1]*

[1] The Novo Nordisk Foundation Center for Biosustainability, Technical University of Denmark, Kongens Lyngby, Denmark, [2] Unibio A/S, Kongens Lyngby, Denmark, [3] Department of Chemical and Biochemical Engineering, Technical University of Denmark, Kongens Lyngby, Denmark

OPEN ACCESS

Edited by:
Marina G. Kalyuzhanaya,
San Diego State University,
United States

Reviewed by:
Jin Wang,
Auburn University, United States
Jeffrey Orth,
Intrexon, United States

***Correspondence:**
Christian Lieven
clie@biosustain.dtu.dk

Specialty section:
This article was submitted to Microbiotechnology, Ecotoxicology and Bioremediation, a section of the journal Frontiers in Microbiology

Received: 23 July 2018
Accepted: 16 November 2018
Published: 04 December 2018

Citation:
Lieven C, Petersen LAH, Jørgensen SB, Gernaey KV, Herrgard MJ and Sonnenschein N (2018) A Genome-Scale Metabolic Model for Methylococcus capsulatus (Bath) Suggests Reduced Efficiency Electron Transfer to the Particulate Methane Monooxygenase. Front. Microbiol. 9:2947. doi: 10.3389/fmicb.2018.02947

Background: Genome-scale metabolic models allow researchers to calculate yields, to predict consumption and production rates, and to study the effect of genetic modifications *in silico*, without running resource-intensive experiments. While these models have become an invaluable tool for optimizing industrial production hosts like *Escherichia coli* and *S. cerevisiae*, few such models exist for one-carbon (C1) metabolizers.

Results: Here, we present a genome-scale metabolic model for *Methylococcus capsulatus* (Bath), a well-studied obligate methanotroph, which has been used as a production strain of single cell protein (SCP). The model was manually curated, and spans a total of 879 metabolites connected via 913 reactions. The inclusion of 730 genes and comprehensive annotations, make this model not only a useful tool for modeling metabolic physiology, but also a centralized knowledge base for *M. capsulatus* (Bath). With it, we determined that oxidation of methane by the particulate methane monooxygenase could be driven both through direct coupling or uphill electron transfer, both operating at reduced efficiency, as either scenario matches well with experimental data and observations from literature.

Conclusion: The metabolic model will serve the ongoing fundamental research of C1 metabolism, and pave the way for rational strain design strategies toward improved SCP production processes in *M. capsulatus*.

Keywords: COBRA, genome-scale metabolic reconstruction, C1 metabolism, single cell protein, methanotrophy, constraint-based reconstruction and analysis

INTRODUCTION

The Gram-negative, obligate-aerobe *Methylococcus capsulatus* (Bath) is a methane oxidizing, gamma-proteobacterium. Since its initial isolation by Foster and Davis (1966), the organism has been subject to a wide array of studies. The global role of *M. capsulatus* as a participant in the carbon cycle has been elucidated (Hanson and Hanson, 1996; Jiang et al., 2010) as well as its effects on

human (Indrelid et al., 2017) and animal health and disease (Kleiveland et al., 2013). Specifically the latter studies have been triggered by a considerable commercial interest in *M. capsulatus* (Bath) as the primary microbe used for the production of Single Cell Protein (SCP) as animal feed starting in the 70 s (Øverland et al., 2010). Now that hydraulic fracturing has made natural gas a cheap and abundant feedstock (Ritala et al., 2017), the application of *M. capsulatus* (Bath) for this purpose is being explored again (Nunes et al., 2016; Petersen et al., 2017). Another portion of studies, however, has focused on uncovering the biochemical and genetic basis of the organism's unique metabolism (Anthony, 1983). Yet, the greatest interest has been the role and function of the initial enzyme in methanotrophy, methane monooxygenase (Ross and Rosenzweig, 2017), responsible for oxidation of methane to methanol.

Methylococcus capsulatus (Bath) is able to express two distinct types of methane monooxygenases: a soluble form of methane monooxygenase (sMMO) and a particulate, or membrane-bound form (pMMO). The expression of these enzymes is strongly influenced by the extracellular concentration of copper; when *M. capsulatus* (Bath) is grown in the presence of low levels of copper the sMMO is active, while the pMMO is predominantly active at high levels. Both enzymes require an external electron donor to break a C-H bond in methane. While the electron donor for the sMMO is NADH (Colby and Dalton, 1978, 1979; Lund et al., 1985; Blazyk and Lippard, 2002), the native reductant to the pMMO has not yet been elucidated due to difficulties to purify the enzyme and assay its activity *in vitro* (Ross and Rosenzweig, 2017). Three hypotheses regarding the mode of electron transfer to the pMMO have been suggested previously:

(1) In the *redox-arm* mode (Dawson and Jones, 1981), the methanol dehydrogenase (MDH) passes electrons via cytochrome c555 (cL) (Anthony, 1992) and cytochrome c553 (cH) (DiSpirito et al., 2004) to either a CBD- or AA3-type terminal oxidase (Larsen and Karlsen, 2016) and thus contributes to building up a proton motive force (PMF) and the synthesis of ATP (**Figure 1**). The electrons required for the oxidation of methane are provided through ubiquinone (Q8H2). Reactions downstream of MDH responsible for oxidizing formaldehyde to CO_2 feed electrons into the Q8 pool. This includes dye-linked formaldehyde dehydrogenase (DL-FALDH), formate dehydrogenase (FDH) and any NAD reducing reactions which ultimately contribute electrons through the NADH dehydrogenases (NDH-1, NDH-2, NQR). See **Figure 1**. Although no binding site has been identified, there is support for pMMO reduction by endogenous quinols (Shiemke et al., 2004).

(2) With the *direct coupling* mode, the MDH is able to directly pass electrons to the pMMO (Wolfe and Higgins, 1979; Leak and Dalton, 1983; Culpepper and Rosenzweig, 2014). Here, cytochrome c555 is the electron donor to the pMMO instead of ubiquinol. This mode is supported by results from cryoelectron microscopy which indicates that the pMMO and the MDH form a structural enzyme complex (Myronova et al., 2006).

(3) The *uphill electron transfer* mode supposes that the electrons from cytochrome c553 can reach the ubiquinol-pool facilitated by the PMF at the level of the ubiquinol-cytochrome-c reductase. This mode was proposed by Leak and Dalton (1986b) as it could explain the observed reduced efficiency.

A genome-scale metabolic model (GEM) not only represents a knowledge base that combines the available physiological, genetic and biochemical information of a single organism (Thiele and Palsson, 2010), but also provides a testbed for rapid prototyping of a given hypothesis (Benedict et al., 2012). Hence, we present the first manually curated GEM for *M. capsulatus* Bath, with the intent of supplying the basis for hypothesis-driven metabolic discovery and clearing the way for future efforts in metabolic engineering (Kim et al., 2015). Using the GEM, we investigate the nature of electron transfer in *M. capsulatus* (Bath) by comparing the model's predictions against experimental data from Leak and Dalton (1986a). Furthermore, we compare its predictions to those of the model of *Methylomicrobium buryatense* 5G(B1) (de la Torre et al., 2015) and explain notable differences by considering the proposed electron transfer modes.

RESULTS AND DISCUSSION

Reconstruction

The presented genome-scale metabolic reconstruction of *M. capsulatus* (Bath) termed iMcBath is based on BMID000000141026, an automatic draft published as part of the Path2Models project (Büchel et al., 2013). The whole genome sequence of *M. capsulatus* (Bath) (GenBank AE017282.2; Ward et al., 2004) was used to aid the curation process and to supply annotations (see section "Materials and Methods"). This metabolic reconstruction consists of 843 enzymatic reactions that interconvert and transport 759 unique metabolites. The total number of reactions, including exchange, demand and the biomass reactions, is 913. The model attributes reactions and metabolites to four distinct compartments: The cytosol, the periplasm, an intramembranous compartment and the medium, which is referred to as extracellular in the model. Gene-Protein-Reaction rules (GPR) associated with 730 unique genes support 86.97% of the included reactions with, leaving 119 reactions without a GPR. The GPRs include representation of 43 enzyme complexes.

The model and all scripts used during reconstruction are made available publicly on Github at https://github.com/ChristianLieven/memote-m-capsulatus. The model is available in the community-standard SMBL format (Level 3 Version 2 with FBC; Olivier and Bergmann, 2015) and a JSON format that is native to cobrapy (Ebrahim et al., 2013).

Biomass Reaction

In stoichiometric models biological growth is represented as the flux through a special demand reaction. The so-called biomass reaction functions as a drain of metabolites, which are either highly reduced non-polymeric macromolecules such as lipids and steroids or precursors to typical biopolymers such as nucleic acids, proteins or long-chain carbohydrates. The stoichiometry of an individual precursor was calculated from the principal composition of *M. capsulatus* (Bath) as reported

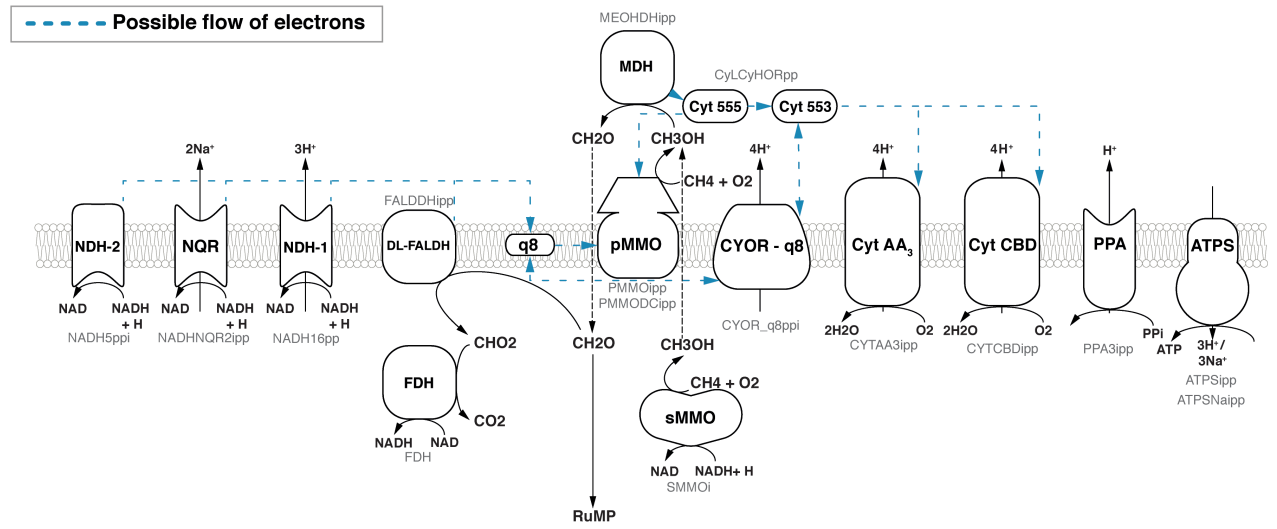

FIGURE 1 | Overview of the respiratory chain in *Methylococcus capsulatus* Bath as implemented in iMcBath. Black text in the center of the symbols denotes the common abbreviation, while the faint gray text below denotes the corresponding reaction ID in the metabolic model. Blue dotted arrows indicate possible flow of electrons between respiratory components. The individual electron transfer modes to the pMMO are outlined in greater detail in **Figure 2**.

by Unibio (2018). The monomer composition of individual macromolecules was calculated from different sources. A detailed account of the resources is provided in the methods section and an overview of the biomass reaction is given in **Supplementary Table 1**.

The growth-associated maintenance (GAM) and the non-growth associated maintenance (NGAM) requirements for *M. capsulatus* are yet to be determined experimentally. Therefore, a GAM value of 23.087 mmol ATP gDW^{-1} h^{-1} was estimated according to Thiele and Palsson (2010) based on the data for *Escherichia coli* published by Neidhardt et al. (1990). The value for GAM is expected to increase with the growth rate of the cells (Varma et al., 1993). Like de la Torre et al. (2015) had done for *M. buryatense* 5G(B1), we assumed the NGAM of *M. capsulatus* (Bath) to be similar to that of *E. coli* thus setting it to 8.39 mmol ATP gDW^{-1} h^{-1} (Feist et al., 2010).

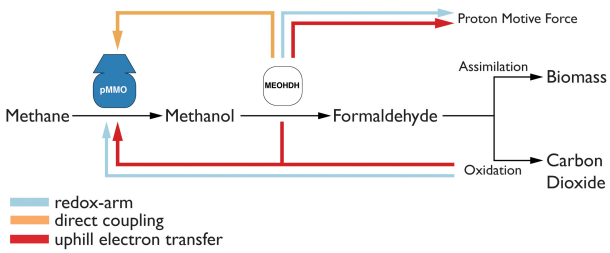

FIGURE 2 | The three possible modes of electron transfer to the pMMO. (1) *Redox-arm*: The methanol dehydrogenase transfers electrons to the terminal oxidase which contributes to increasing the proton motive force (PMF), while the pMMO draws electrons from the quinone pool. (2) *Direct coupling*: Electrons from the oxidation of methanol are transferred directly to the pMMO. (3) *Uphill electron transfer*: Electrons from the methanol dehydrogenase feed back into the ubiquinol-pool.

Metabolism

To study which of the three modes of electron transfer is active in *M. capsulatus* (Bath), they were each implemented in the model. The implementation is illustrated in **Figure 2**. To include the *redox-arm* we implemented the reaction representing the particulate methane monooxygenase, in the model termed as PMMOipp, utilizing Q8H2 as a cofactor. Accordingly, a variant of the pMMO reaction was added to account for a possible direct coupling to the MDH. In this variant reaction, termed PMMODCipp, the cofactor is cytochrome c555, represented as the metabolite focytcc555_p in the model. To enable an *uphill electron transfer*, the reaction representing the ubiquinol-cytochrome-c reductase (CYOR_q8ppi in the model), was constrained to be reversible while keeping PMMOipp active.

Following the path of carbon through metabolism downstream from the MDH, the model includes both the reaction for a ubiquinone-dependent formaldehyde dehydrogenase (Zahn et al., 2001), termed FALDDHipp, and an NAD-dependent version, termed ALDD1 (**Figure 3**). Despite of the initial evidence for the latter reaction (Tate and Dalton, 1999) having been dispelled by Adeosun et al. (2004), it was added to allow further investigation into the presence of a putative enzyme of that function. An additional pathway for formaldehyde oxidation represented in both genome and model is the tetrahydromethanopterin(THMPT)-linked pathway (Vorholt, 2002).

Formaldehyde assimilation in *M. capsulatus* (Bath) occurs primarily through the ribulose monophosphate (RuMP)-pathway. As outlined by Anthony (1983), the RuMP-pathway has four hypothetical variants. Based on the annotated genome published by Ward et al. (2004), we identified

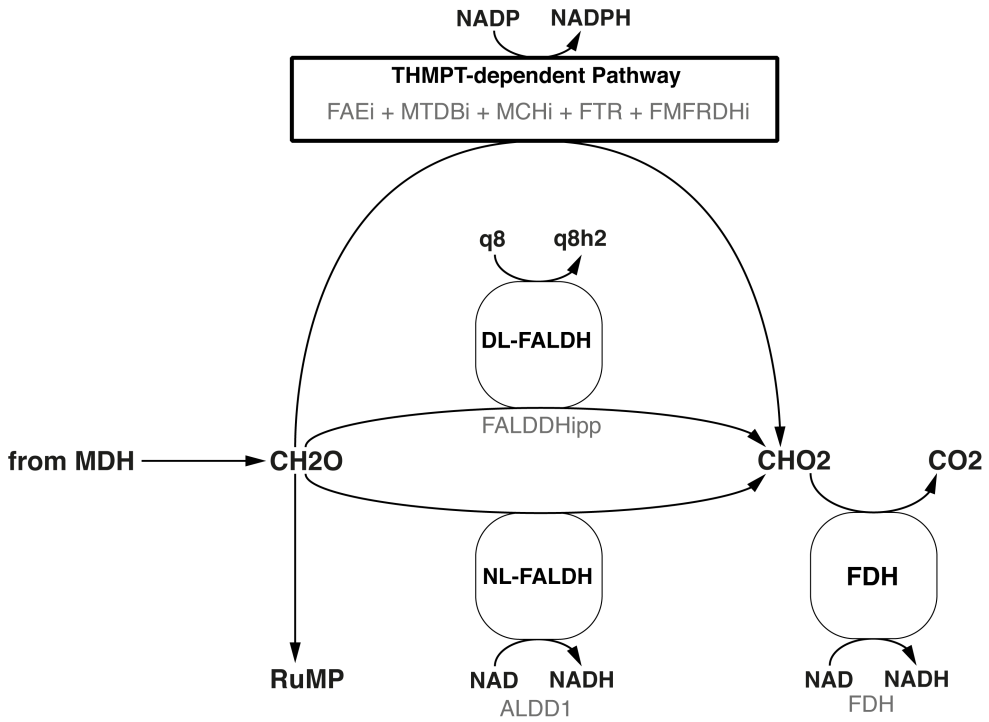

FIGURE 3 | Three different formaldehyde oxidation pathways are represented in the model. Black text denotes the common name, while faint gray text denotes the reaction ID in the metabolic model.

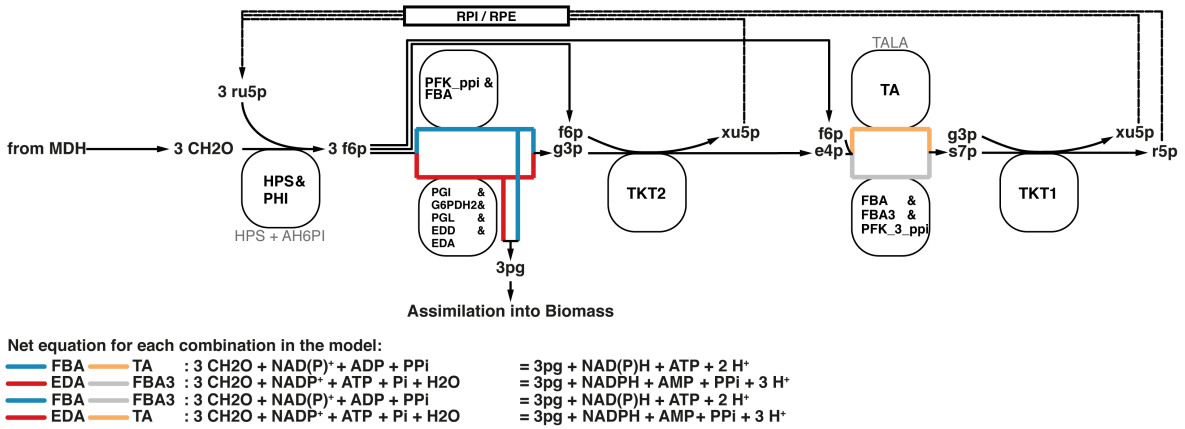

FIGURE 4 | All four variants of the RuMP pathway are represented in the metabolic model. If there is a common enzyme name the black text denotes the common name, while faint gray text denotes the reaction ID in the metabolic model. Otherwise the black text is also the reaction ID in the model.

not only both C6 cleavage pathways depending either on the 2-keto, 3-deoxy, 6-phosphogluconate (KDPG) aldolase (EDA) or the fructose bisphosphate aldolase (FBA), but also the transaldolase (TA) involved in the rearrangement phase that regenerates ribulose 5-phosphate. The alternative to a transaldolase-driven rearrangement step is the use of a sedoheptulose bisphosphatase, which was not included in the initial annotation. Strøm et al. (1974) could not detect specific activity using cell-free preparations. Yet, we decided to add a corresponding reaction for two reasons. First, the FBA has been characterized to reversibly catalyze sedoheptulose bisphosphate cleavage (Rozova et al., 2010), which is reflected by the reaction FBA3 in the model. Second, the pyrophosphate-dependent 6-phosphofructokinase (PFK_3_ppi) was reported to have higher affinity and activity to the reversible phosphorylation of seduheptulose phosphate than compared to fructose 6-phosphate (Reshetnikov et al., 2008). Thus, all of the resulting four combinations that make up the RuMP-pathway are represented in this metabolic model (**Figure 4**).

The genome of *M. capsulatus* (Bath) encodes genes for a complete Calvin Benson Bassham (CBB) cycle (Taylor, 1977; Taylor et al., 1980; Baxter et al., 2002) and a partial Serine pathway for formaldehyde assimilation (Ward et al., 2004). It was argued by Taylor et al. (1981) that *M. capsulatus* (Bath) can metabolize glycolate [a product of the oxygenase activity of the ribulose bisphosphate carboxylase (RBPC)] via this pathway. Both Taylor and Ward, further suggested the presence of unique key enzymes to complete the Serine pathway, such as hydroxymethyl transferase, hydroxypyruvate reductase and malate-CoA lyase. However, since the gene annotation did not reflect this and the RuMP pathway is reportedly the main pathway for formaldehyde assimilation (Kelly et al., 2005), these putative reactions were not included.

All genes of the TCA cycle were identified in the genome sequence and all associated reactions were included accordingly (Ward et al., 2004). Because no activity of the 2-oxoglutarate dehydrogenase has so far been measured *in vivo* (Wood et al., 2004; Kelly et al., 2005), the associated reactions have been constrained to be blocked (both lower and upper bounds were set to zero). This way they can easily be activated if needed. For instance, if a growth condition is discovered where activity for this enzyme can be detected.

Based on reactions already present in BMID000000141026, the information in the genome annotation, and the measured biomass composition, we curated the biosynthetic pathways of all proteinogenic amino acids, nucleotides, fatty acids, phospholipids, panthothenate, coenzyme A, NAD, FAD, FMN, riboflavin, thiamine, myo-inositol, heme, folate, cobalamine, glutathione, squalene, lanosterol, peptidoglycan. Since no corresponding genes could be identified, reactions catalyzing the biosynthesis of lipopolysaccharide (LPS) were adopted from iJO1366 (Orth et al., 2011) under the assumption that the biosynthesis steps among gram-negative bacteria require amounts of ATP comparable to *E. coli*.

Methylococcus capsulatus (Bath) is able to metabolize the nitrogen sources ammonium (NH_4) and nitrate (NO_3) in a variety of ways. When the extracellular concentration of NH_4 is high (>1 mM), alanine dehydrogenase (ADH) is the primary pathway for nitrogen assimilation into biomass, when it is low (<1 mM) assimilation is carried out via the glutamine synthetase/glutamine synthase (GS/GOGAT) pathway (Murrell and Dalton, 1983). In addition to assimilation, the two monooxygenases are able to oxidize ammonium to hydroxylamine (Colby and Dalton, 1978; Bédard and Knowles, 1989), which is then further oxidized by specific enzymes first to nitrite (Bergmann et al., 1998; **Figure 5**), and even to dinitrogen oxide (Campbell et al., 2011). NO_3 is reduced to NH_4 via nitrite and ultimately assimilated via GS/GOGAT. Furthermore, it has been shown that *M. capsulatus* (Bath) is able to fix atmospheric nitrogen (N_2) (Murrell et al., 1983). The nitrogenase gene cluster has been identified (Oakley and Murrell, 1991) and annotated accordingly (Ward et al., 2004), and the corresponding reactions have been included in the model. As the enzyme has not yet been specifically characterized, the nitrogenase reaction was adapted from iAF987 (Feist et al., 2014). A schema showing these reactions side-by-side is displayed in **Figure 6**.

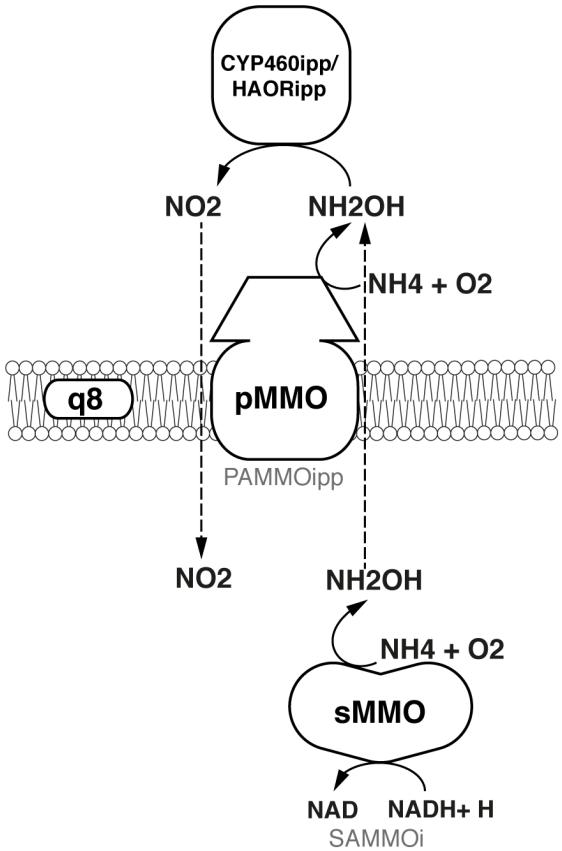

FIGURE 5 | Oxidation of ammonia to nitrite.

A metabolic map of all the reactions in the model was built using Escher (King et al., 2015) and is available as **Supplementary Figure 1**.

Prediction of Transport Reactions

As a last step we added transport reactions that were not in the draft reconstruction. Inferring membrane transport reactions from the genome sequence is difficult, as usually the precise 3D structure of transport proteins dictates which metabolite classes can be transported (Mishra et al., 2014). Even if the substrates are known, the energy requirements of transport are often undefined. Working on protein sequence matches using PsortB 3.0 (Yu et al., 2010), combined with BLAST (Altschul et al., 1990) matches against TransportDB (Elbourne et al., 2017) and the Transporter Classification Database (TCDB) (Saier et al., 2006), we were able to identify 56 additional transport reactions. We have limited the number of transporters to be added, focusing specifically on transporters with known mechanisms and transport of metabolites already included in the model. A list of putative transport-associated genes that we did not consider is available at https://github.com/ChristianLieven/memote-m-capsulatus. Ward et al. (2004) hypothesized that some of these genes may facilitate the uptake of sugars for growth. Kelly et al. (2005) argue that these genes instead may allow a

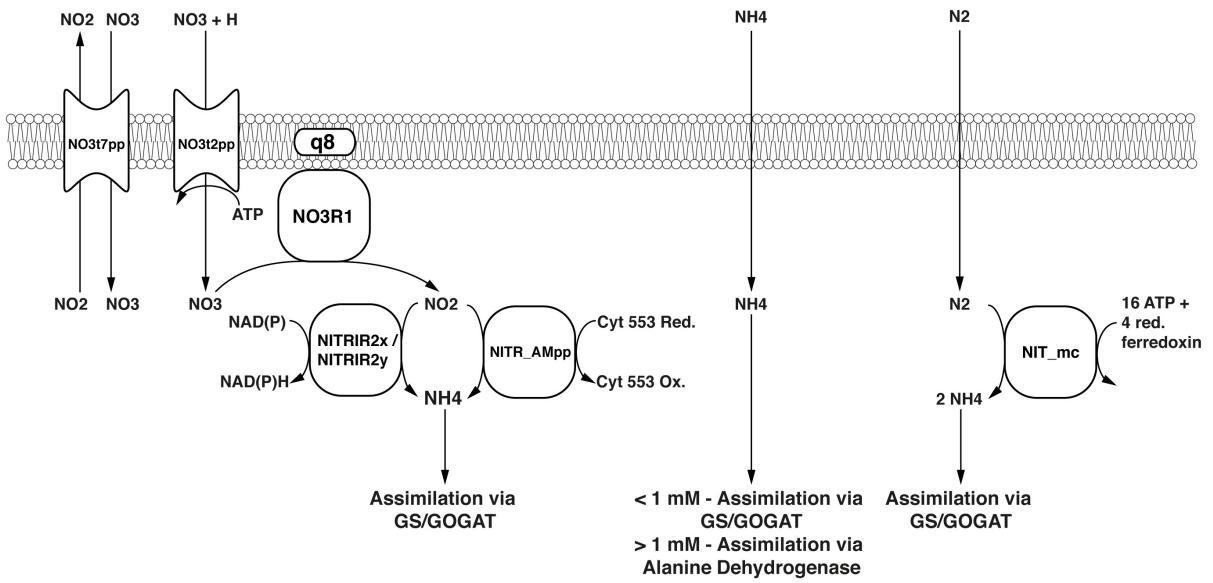

FIGURE 6 | Nitrogen assimilation and fixation pathways represented in the model. Black text in the center of the symbols denotes reaction IDs. Common names are used for metabolites.

function similar to *Nitrosomas europaea*, which is able grow on fructose as a carbon-source with energy from ammonia oxidation (Hommes et al., 2003; Kelly et al., 2005). Thus, this list is a good starting point to study potential alternate carbon source use by *M. capsulatus* (Bath).

Parameter Fitting to Determine the Mode of Electron Transfer

To determine which combination of the three aforementioned electron transfer modes is active in *M. capsulatus* (Bath), we constrained the model based on experiments conducted by Leak and Dalton (1986a). Since the three modes relate to how the pMMO receives electrons, we focused on the data generated by growing *M. capsulatus* (Bath) in high-copper medium, which is the condition in which pMMO is predominantly active. We used the average of carbon and oxygen-limited measurements as a reference. Having constrained the model, we compared the Leak and Dalton's measurements for the ratio of oxygen consumption to methane consumption (O_2/CH_4) to the predictions of the model (**Figure 7**). We considered the O_2/CH_4 ratio to be a key metric for the respiratory chain in *M. capsulatus* (Bath), as it is a function of the mode of electron transfer to the pMMO. The central carbon metabolism was left unconstrained.

Under the assumption that the mode of electron transfer to pMMO would be independent of the source of nitrogen, we compared the O_2/CH_4 ratios of the model constrained to employ one of the three modes of electron transfer exclusively to the corresponding reference values of *M. capsulatus* (Bath) grown on either NO_3 or NH_4. However, neither of the modes adequately represented the measured O_2/CH_4 ratios of about 1.43 and 1.6, respectively. Although Leak and Dalton had proposed that the *reverse* or *uphill electron transfer* is the most probable mode (Leak and Dalton, 1986b), the model predictions allowing for an unbounded *uphill transfer* did not support this (**Figure 7E**), as the efficiency was almost comparable to predictions using *direct coupling*.

We altered the efficiency of the three modes to determine whether the fit could be improved. For the *redox arm*, we gradually decreased the mol protons required for the synthesis of 1 mol ATP, thereby improving the efficiency. This did not change the O_2/CH_4 ratio (see **Figure 7A**). de la Torre et al. (2015) constructed a GEM for *M. buryatense* 5G(B1) to investigate growth yields and energy requirements in different conditions. Similar to the results presented herein, they found that the *redox-arm* mode correlated least with their experimental data for *M. buryatense*.

We decreased the efficiency of the *direct coupling* mode (PMMODCipp) by forcing a portion of the flux through the regular pMMO reaction (PMMOipp) using ratio constraints (**Figure 7B**). To achieve a ratio representing the measured value of 1.43 required a large decrease in efficiency with almost 85% of the incoming carbon routed through the regular pMMO reaction (see **Supplementary Table 2**). Lastly, we iteratively constrained the lower bound of the reaction associated with the ubiquinol-cytochrome-c reductase (CYOR_q8ppi), to reduce the efficiency of the *uphill-electron transfer* (**Figure 7C**).

Leak and Dalton (1986b) developed mathematical models for each mode based on previous calculations (Harder and Van Dijken, 1976; Anthony, 1978). Their models lead them to conclude that both *direct coupling* and *uphill electron transfer* operating at reduced efficiency may account for the observed high ratios of O_2/CH_4, which agrees with our predictions. Since experimental

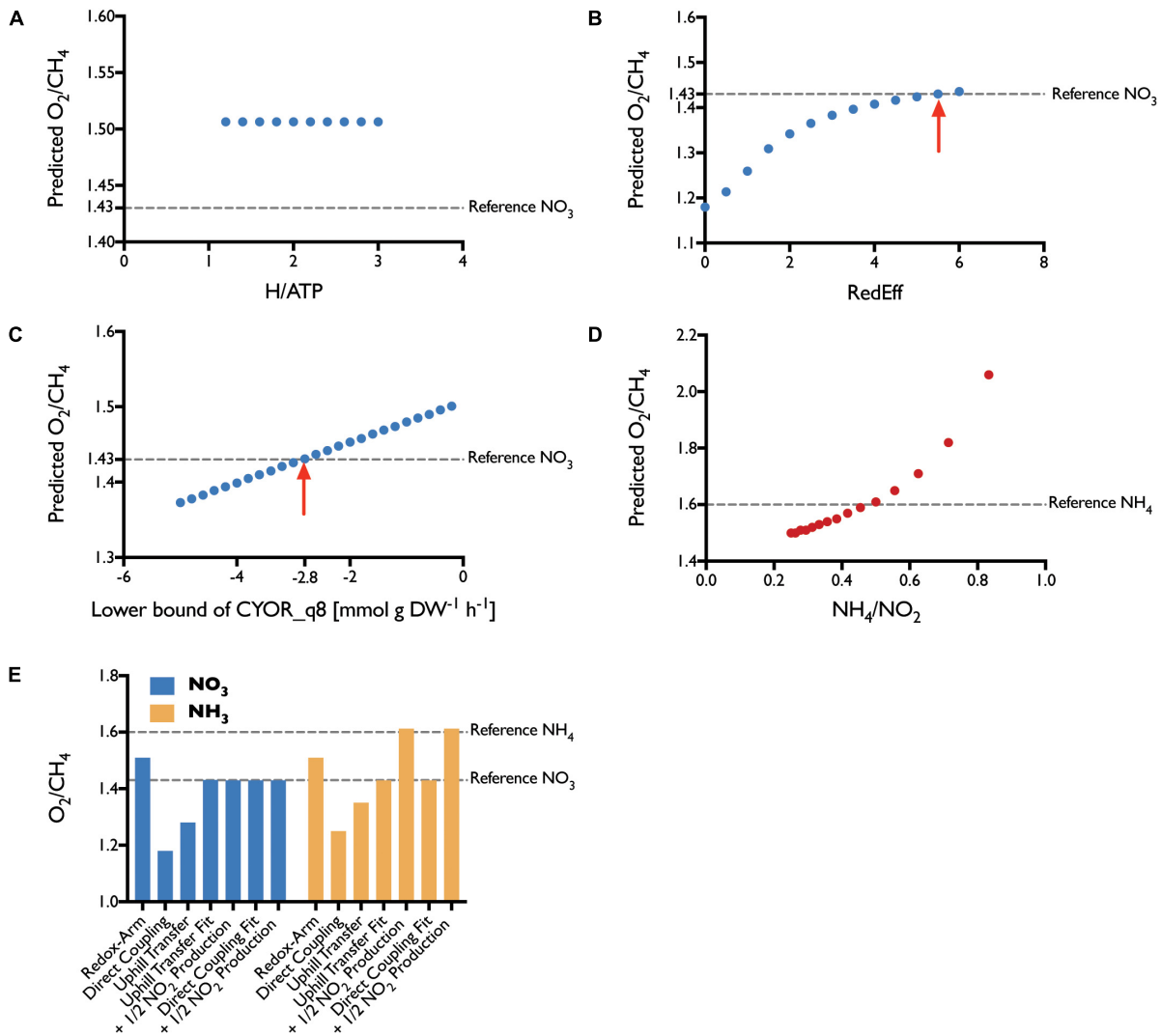

FIGURE 7 | Parameter Fit. The efficiency of each transfer mode was varied iteratively to determine the best fit. **(A)** For the *redox-arm* mode we varied the ratio of protons required per synthesis of 1 mol ATP, with no effect. **(B)** Fitting the *direct-coupling* mode, we forced a portion of the flux through the PMMOipp reaction. The red arrow marks the best fit with 5.5 times more carbon flux through PMMOipp than PMMODCipp. **(C)** The *Uphill-electron transfer* was fit by allowing reverse flux through the ubiquinol-cytochrome c reductase (CYOR_q8) reaction. The red arrow marks the best fit at a lower bound of **–**2.8 mmol g DW^{-1} h^{-1}. **(D)** To account for energy loss through NH_3 oxidation, several ratios of NH_4 uptake to NO_2 production were considered. The closest fit was achieved with a ratio of around 0.5. **(E)** Without reducing electron transfer efficiency none of the modes could fit the reference value for NO_3. For NH_3, the reference was met after accounting for the effect of NH_3 oxidation to NO_2. Reduced efficiency *uphill electron transfer* and *direct coupling* both allow prediction of O_2/CH_4 ratios that agree well with the literature reference.

results on the nature of protein–protein interactions between pMMO and MDH seem to be inconclusive (Myronova et al., 2006; Culpepper and Rosenzweig, 2014; Ross and Rosenzweig, 2017), neither of the modes can be ruled out entirely.

Parameter Fitting to Determine the Impact of NH_4 Oxidation

Leak and Dalton pointed out, that the unexpectedly high O_2/CH_4 ratio of 1.6 was the product of latent NH_4 oxidation rather than assimilation leading to elevated levels of NO_2 which detected at medium concentrations of around 200 μM (Leak and Dalton, 1986a). They were uncertain whether this increase in the ratio of O_2/CH_4 could be attributed to the energetic burden of oxidizing NH_4 or an uncoupling effect of NO_2.

To investigate this effect, we introduced a ratio constraint (see Methods) coupling the uptake of NH_4 to the excretion of NO_2 and explored a number of values for this ratio (**Figure 7C**). According to the simulations, the energy spent oxidizing about 50% of incoming NH_4 to NO_2 is sufficient to account for the observed, high O_2/CH_4 ratio of 1.6. Although this shows that the loss of energy could be significant enough to account for the increased ratio, this does not exclude a potential combined effect because of energy decoupling.

Regardless it shows that calculations using the metabolic model can accurately reflect the *in vivo* behavior of *M. capsulatus* (Bath).

Validation of the Model

Specific growth rates of 0.25 and 0.37 h^{-1} were measured by Joergensen and Degn (1987) for *M. capsulatus* (Bath) on copper-free and copper-rich NO_3 mineral salt medium, respectively. Simulations of iMcBath with an active sMMO reaction yielded 0.19 h^{-1} on NO_3 and 0.26 h^{-1} on NH_4 as the nitrogen source, as well as 0.20 h^{-1} for growth driven by the pMMO on NO_3 and 0.30 h^{-1} on NH_4. The predicted growth rates scale together with the uptake rates for methane and the respective nitrogen sources. The uptake rate for methane in iMcBath was constrained to 18.46 mmol $g_{DW}{}^{-1}$ h^{-1}, a value adopted from de la Torre et al. (2015) due to the lack of a specific measurement for *M. capsulatus* (Bath). Uptake rates for NO_3 and NH_4 have been left unconstrained for the same reasons. An adjustment of the scale will be possible as soon as these data become available.

The model qualitatively agrees with a report from Patel and Hoare (1971), who determined that *M. capsulatus* (Bath) is capable of using certain amino acids as sources for nitrogen (**Table 1**). Although the transport reactions for these amino acids could not be inferred, the addition of corresponding boundary reactions sufficed to predict growth using FBA. However, the predicted growth rates are not comparable as it seems that in the model some of the carbon is assimilated as the amino acids are ultimately converted into pyruvate. On L-glutamate and L-glutamine as N-sources the model further predicts the production of alpha-ketoglutarate, and on L-valine that of alpha-ketoisovalerate. This is in accordance with findings by Patel and Hoare (1971).

TABLE 1 | Model validation against experimental conditions from literature.

Growth condition	Predicted growth rate [h^{-1}]	Measured growth rate [h^{-1}]
sMMO – NO_3	0.18	0.12[1]
sMMO – NH_4	0.23	0.09[1]
sMMO – L-Alanine	1.0	0.08[1]
sMMO – L-Aspartate	1.0	0.11[1]
sMMO – L-Asparagine	1.0	0.11[1]
sMMO – L-Cysteine	1.0	0.09[1]
sMMO – L-Glutamate	0.47	0.11[1]
sMMO – L-Glutamine	0.47	0.11[1]
sMMO – L-Valine	0.46	0.07[1]
Growth condition	**Predicted growth rate [h^{-1}]**	**Experimental observation**
$CO_2 + H_2 - NO_3$	0.05	Growth observed[2]
$CO_2 - NO_3$	Infeasible	No growth[2]
$H_2 - NO_3$	0	No growth[2]
CO_2 + Formate – NO_3	0.06	Growth observed[2]
Formate – NO_3	0.06	No growth[2]

[1]*Patel and Hoare (1971) converted from Doubling Time [h^{-1}]*, [2]*Baxter et al. (2002).*

To further validate iMcBath, we simulated autotrophic growth on carbon dioxide and molecular hydrogen (H_2) as observed previously by Baxter et al. (2002). Indeed, growth was possible using carbon dioxide as the C-source and H_2 as the source of energy (**Table 1**). Replacement of H_2 with formate also allowed the production of biomass, although formate is both assimilated and oxidized. This is because the model allows for the consumption of cytosolic carbon dioxide created as the end-product of formate oxidation. In addition to the ribulose-bisphosphate carboxylase converting CO_2 to 3-phosphoglycerate, this mode of operation relies on the pyrophosphate-dependent 6-phosphofructokinase (PFK_3_ppi) to reversibly convert sedoheptulose-1,7-bisphosphate to sedoheptulose-7-phosphate and fructose bisphosphate to fructose-6-phosphate thus providing these intermediates to the RuMP cycle (Reshetnikov et al., 2008). Growth just on carbon dioxide or molecular hydrogen exclusively could not be simulated as reported by the authors.

Flux balance analysis confirms the results from Stanley and Dalton (1982) predicting latent CO_2 fixation even during growth on methane.

Comparison With Other Models

We compared iMcBath, the preceding automated draft reconstruction BMID000000141026, and a GEM of the gram-negative, gamma-proteobacterium *M. buryatense* strain 5G(B1) (de la Torre et al., 2015) to illustrate how much the model has progressed from the draft through manual curation and how the mode of electron transfer affects growth parameters within the group of gamma-proteobacteria (see **Table 2**).

Unsurprisingly, the automated draft generally performs quite poorly in comparison with the curated models. It's not possible to produce biomass from methane, even in rich media conditions, which is indicative of gaps in the pathways leading toward individual biomass components. Moreover, ATP can be produced without the consumption of substrate, which in turn means that key energy reactions are not constrained thermodynamically to have the correct reversibility. In the draft, 51% of the reactions are not supported by Gene-Protein-Reaction rules (GPR), while in iMb5G(B1) this percentage is only 32% and in iMcBath the percentage of these reactions is under 20%. GPRs allow modelers to distinguish between isozymes and enzyme complexes by connecting gene IDs either through boolean "OR" or "AND" rules. In iMcBath, 25 complexes in total were curated and formulated as GPR. Neither the draft model nor iMb5G(B1) make this distinction.

In the automated draft, the oxidation of methane was only possible through a reaction representing the sMMO (MNXR6057). In iMcBath, this was corrected by also implementing reactions that represent the pMMO, one with ubiquinone as the electron donor (PMMOipp), and another that receives electrons from the MDH (PMMODCipp). *M. capsulatus* (Bath), like *M. buryatense 5G*(B1), expresses both the soluble and the particulate monooxygenase depending on the availability of copper in the medium. In iMb5G(B1), however, only the particulate monooxygenase is represented by the reaction "pMMO." The ability of *M. capsulatus* (Bath) to

TABLE 2 | Model Comparison.

	iMcBath	BMID000000141026	iMb5G(B1)
Structure			
Methane oxidation	SMMOi, PMMOipp, PMMODCipp	MNXR6057	pMMO
Growth on N-sources	Urea, NO_2, NO_3, NH_4, N_2, Ala, Asn, Asp, Cys, Gln, Glt, Val	No Growth	NO_3
Performance			
ATP Production closed exchanges	False	True	False
ATP Production rate – NH_4	0.775	1000	1
ATP Production rate – NO_3	0.365	1000	0.519
Growth rate – pMMO – NH_4	0.300	No growth	0.34
Growth rate – pMMO – NO_3	0.205	No growth	0.27
O_2/CH_4 Ratio – pMMO – NH_4	1.434	No growth	1.156
O_2/CH_4 Ratio – pMMO – NO_3	1.430	No growth	1.116
Specifications			
Reactions without GPR	119	950	129
Enzyme complexes	43	0	0
Total # genes	730	589	313
Total # metabolites	879	935	403
Total # reactions	913	1858	402

The presented reconstruction iMcBath, the automated draft BMID000000141026 and iMb5G(B1), a genome-scale reconstruction of Methylomicrobium buryatense strain 5G(B1).

grow on ammonia, nitrate and nitrogen has been characterized experimentally (Murrell and Dalton, 1983). In addition to that, however, iMcBath also predicts growth on nitrite and urea. Nitrite is an intermediate in the assimilation of nitrate, yet also reported to elicit toxic effects (Leak and Dalton, 1986a; Nyerges and Stein, 2009), hence *in vivo* growth may only be possible on low concentrations. Growth on urea is possible in the model since we identified *MCA1662* as an ATP-driven urea transporter and gap-filled a urease reaction when curating the cobalamine biosynthesis pathway. As a consequence of this, urea can be taken up into the cytosol and broken down into ammonia and carbon dioxide, the former of which is then assimilated. Further experimental work is necessary to verify this *in vivo*. *M. buryatense* 5G(B1) is reported to grow on nitrate, ammonia and urea, yet without adding the respective transport reactions iMb5G(B1) only grows on nitrate. While the draft model for *M. capsulatus* (Bath) contains exchange reactions for all the tested nitrogen sources except for urea, it couldn't grow at all, which again is likely because of gaps in the pathways leading to biomass precursor metabolites.

The difference between *M. capsulatus* (Bath) and *M. buryatense* 5G(B1) becomes apparent when comparing the growth energetics of iMcBath and iMb5G(B1). iMb5G(B1) produces more mmol gDW^{-1} h^{-1} ATP than iMcBath. Because of this the hypothetical growth-rates predicted by iMb5G(B1) are higher than those of iMcBath regardless of the respective nitrogen source. This difference is likely a direct consequence of the mode of electron transfer to the monooxygenase and thus the efficiency of the methane oxidation reaction in total. When comparing the ratio of the uptake rate of oxygen and the uptake rate of methane for the two models, we can see that the resulting values in iMb5G(B1) are lower than in iMcBath. It was recently reported, that instead of the reverse-electron transfer and redox-arm mode active in *M. capsulatus* (Bath), a mixture of *direct coupling* from pMMO to MDH and *reverse electron transfer* seems to be the most likely mode in *M. buryatense* 5G(B1) (de la Torre et al., 2015).

CONCLUSION

iMcBath is the first, manually curated, GEM for *M. capsulatus* (Bath). With iMcBath, we combine biochemical knowledge of half a century of research on *M. capsulatus* (Bath) into a single powerful resource, providing the basis for targeted metabolic engineering, process design and optimization, omic-data contextualization and comparative analyses. We applied the metabolic model to study the complex electron transfer chain of *M. capsulatus*, by analyzing the three modes of electron transfer that had been proposed previously (Leak and Dalton, 1986b). We did so by corresponding each mode with the flux through a reaction in the model, and consequently comparing the predicted O_2/CH_4 ratios to experimentally measured values by Leak and Dalton (1986a). Simulation and experiment agreed either when the model was constrained to employ the *uphill electron transfer* at reduced efficiency or *direct coupling* at strongly reduced efficiency for *M. capsulatus* (Bath) grown *in silico* on NO_3 as the source of nitrogen. Further experimental validation is required as neither mode can be ruled out exclusively. The experimentally observed effect of NH_4 oxidation to NO_2 could be replicated by considering the energy burden alone.

Future applications of the metabolic model could include hypothesis testing of the regulation of the MMO in other growth conditions (Kelly et al., 2005), studying the effects of the predicted hydrogenases on the energy metabolism of *M. capsulatus* (Bath) (Ward et al., 2004), and exploring venues of metabolic engineering for an improved production of metabolites (Kalyuzhnaya, 2016). Improved validation of the model requires more experimental data, which is surprisingly sparse. Specific uptake and growth rates in various conditions, as well as gene deletion studies are paramount to improving iMcBath. The authors would like to reach out to any experts on *M. capsulatus* to get involved in maintaining and improving iMcBath. The model and additional data is hosted publicly on Github[1]. Any

[1]https://github.com/ChristianLieven/memote-m-capsulatus

contributions are welcome regardless of whether they come in the form of pull requests, issues, comments, or suggestions.

MATERIALS AND METHODS

Model Curation

Starting reconstruction on the basis of an automated draft required additional effort to be able to use it for calculations. The automated draft used two sets of ID namespaces, BiGG (King et al., 2016) and MetaNetX (MNX) (Ganter et al., 2013). Hence, the first step in the curation efforts consisted of unifying the namespace by mapping all metabolite and reaction identifiers from MNX into the human-readable BiGG namespace. Individual metabolites and reactions with unmappable IDs, that could not be identified in the BiGG database and for which there was little evidence in the form of GPR rules, were removed from the model. Several metabolite formulas contained polymer units, and many reactions lacked EC numbers. Using the MNX spreadsheet exports "chem_prop.tsv" and "reac_prop.tsv" from version 1.0 (Bernard et al., 2014) and 2.0 (Moretti et al., 2016) most of these issues were resolved. Due to said malformed and missing metabolite formulae, many reactions were not mass-charge-balanced. We used the "check_mass_balance" function in cobrapy (Ebrahim et al., 2013) to identify and balance 99.4% of the reactions in the model. The remaining five reactions, belonging to fatty acid biosynthesis, involve a lumped metabolite that represents the average fatty acid content of *M. capsulatus* (Bath).

After mapping the reaction and metabolite identifiers from the MetaNetX namespace to the BiGG namespace, we proceeded with the curation efforts as follows: First, we chose a subsystem of interest, then we picked a pathway and using information from either the genome sequence, published articles, the metacyc or uniprot databases, and lastly, we enriched each enzymatic step in said pathway with as much information as possible. Information that was added included for instance: GPR, reaction localization, EC numbers, a confidence score, possible cofactors and inhibitors and cross references to other databases such as KEGG, BIGG and MetaNetX. For each metabolite involved in these reactions, we defined the stoichiometry, charge and elemental formula, either based on the corresponding entries in the BiGG database or on clues from literature.

If reactions from a pathway were present in the draft, we checked their constraints and directionality, consulting the corresponding reactions in MetaCyc (Caspi et al., 2014). This was necessary as many of the irreversible reactions in the draft reconstruction seemed to have been "inverted" when compared to the corresponding reactions in the reference databases, which made flux through them impossible in normal growth conditions.

The energy metabolism and methane oxidation were curated first. Except for the reaction representing the sMMO, all reactions were newly constructed, as they were absent in the draft. Then, in order to achieve sensible FBA solutions for growth on methane, the central carbon metabolism, amino acid and nucleotide biosynthesis pathways were manually curated. Simultaneous to the manual curation a metabolic pathway map was created in Escher, which helped us to maintain a visual checklist of curated pathways.

The automated draft contained a rudimentary, generic biomass reaction, which only accounted for the production of proteins, DNA and RNA, but not for the biosynthesis of a cell wall and cell membrane, the maintenance of a cofactor pool, the turnover of trace elements or the energetic costs associated with growth. After calculating a more specific biomass composition for *M. capsulatus* (Bath), further pathway curation was necessary to achieve growth *in silico*. This included the biosynthesis pathways of fatty acids (even, odd and cyclopropane varieties), phospholipids, coenzyme A, Ubiquinol, Lanosterol, FAD, FMN, Riboflavin, NAD and NADP, Heme, Glutathione, Cobalamin, Thiamine, Myo-Inositol, and Lipopolysaccharides. The corresponding biosynthetic pathways were gap-filled and manually curated. To identify the appropriate pathways, MetaCyc pathway maps from the *M. capsulatus* (Bath) specific database were used to compare the reactions that were present in the draft reconstruction[2].

To account for the reported differences in ammonia assimilation of *M. capsulatus* (Bath) when grown in the presence of excess ammonia versus the growth on either atmospheric nitrogen or nitrate, we curated the nitrogen metabolism including the oxidation of ammonia to nitrite via hydroxylamine, the reduction of nitrate and nitrite, the glutamine synthetase/ glutamate synthase reactions and the ADH. Reversible degradation reactions producing ammonia that would potentially bypass the characterized ammonia assimilation pathways were constrained to be irreversible accordingly.

After we had enriched the annotations already in the draft with annotations from the metabolic models iJO1366 (Orth et al., 2011), iRC1080 (Chang et al., 2011), iJN678 (Nogales et al., 2012), and iHN637 (Nagarajan et al., 2013), they were converted into a MIRIAM-compliant format. As a final step, we manually added transport reactions to reflect the uptake energetics of cofactors.

Throughout the reconstruction process, we iteratively tested and validated the reconstruction. For instance, we checked the mass and charge balance of each reaction, attempting to manually balance those that weren't balanced. In the majority of cases metabolites were missing formula or charge definitions. In order to remove energy generating cycles, problematic reactions were manually constrained to be irreversible. Validation was carried out against growth data (Leak and Dalton, 1986a), which was also the point of reference for the parameter fitting.

Biomass Composition

For the principal components of biomass, measurements were made available through the website of our collaborators Unibio (2018). This included specifically the content of RNA (6.7%), DNA (2.3%), crude fat (9.1%), and glucose (4.5%) as a percentage of the cell dry weight. We did not use the percentage values for crude protein (72.9%) and N-free extracts (7.6%) as these measurements are fairly inaccurate relying on very generalized factors. The percentage value of Ash 550 (8.6%) measurements

[2]https://biocyc.org/organism-summary?object=MCAP243233

was inconsistent with the sum of its individual components (4.6%) and was hence excluded.

On the homepage of Unibio, we were also able to find g/kg measurements of all amino acids except for glutamine and asparagine, trace elements and vitamins, which could directly be converted into mmol/g DW. However, we omitted some of data: The stoichiometries for Selenium, Cadmium, Arsenic, Lead, and Mercury were not included in the biomass reaction as their values were negligibly small. Beta-Carotene (Vitamin A) and Gama-Tocopherol (Vitamin E) were omitted because no genes were found supporting their biosynthesis, in addition to both being reportedly below the detection limit (Øverland et al., 2010).

For the lack of better measurements, and assuming that *M. buryatense* and *M. capsulatus* (Bath) are more similar than *M. capsulatus* (Bath) and *E. coli*, the stoichiometries of glutamine and asparagine, intracellular metabolites such as ribulose-5-phosphate, organic cofactors such as coenzyme A, and cell wall components such as LPS were introduced from de la Torre et al. (2015).

Using the GC content calculated from the genome sequence (Ward et al., 2004) and the percentage measurements from Unibio for RNA and DNA, we were able to calculate the stoichiometries of all individual nucleobases.

Unibio's measurements that 94% of the crude fat portion were fatty acids conflicted with previously published results, which indicated that in fact phospholipids are likely to be the main lipid component in *M. capsulatus* (Bath) (Makula, 1978; Müller et al., 2004). Thus, we assumed 94% of the crude fat to be phospholipids. This meant that 6% of the crude fat was composed of fatty acids, the distributions of which were again provided by Unibio. However, in order to calculate the stoichiometry of each fatty acid we recalculated the distribution to exclude the unidentified part. Makula had also measured the composition of the phospholipid pool itself (Makula, 1978), from which we calculated the corresponding stoichiometries for phosphatidylethanolamine, phosphatidylcholine, phosphatidylglycerol, and cardiolipin.

Bird et al. (1971) had reported the percentage of squalene and sterols of dry weight, which we converted into mmol/g DW without further corrections. Since the genes for hopanoid synthesis were identified we included diplopterol in the biomass reaction (Ward et al., 2004; Nakano et al., 2007). For a lack of more detailed measurements we estimated a similar contribution to the overall composition as squalene. We specifically used lanosterol to represent the general class of sterols in the biomass reaction, since we had only been able to reconstruct the synthesis pathway of lanosterol and since lanosterol is a key precursor metabolite in the biosynthesis of all other sterols.

The growth associated maintenance (GAM) energy requirements were calculated in accordance with protocol procedures outline in **Figure 13** of Thiele and Palsson (2010). The final value of 23.087 mmol ATP g_{DW}^{-1} h^{-1} is the sum of the amount of ATP required to synthesize the proportional content of proteins, DNA and RNA per one gram of cell dry weight (DW). For each component *i* we obtained the synthesis energy coefficient *C* [mmol ATP/ mmol component] from Thiele and Palsson (2010), who calculated them based on Tables 5 and 6 of Chapter 3 in Neidhardt et al. (1990). With x denoting the amount of a specific component $\boldsymbol{i}$ per gram DW [mmol component/ g_{DW}], the following formula determines the GAM requirement:

$$\sum_{i=1}^{n} (x_i C_i) \quad (1)$$

Specifically, the coefficients used herein are $C_P = 4.324$, $C_D = 1.365$, $C_R = 0.406$ and $x_P = 5.312$, $x_D = 0.047$, $x_R = 0.135$.

Transport Reactions

The identification of transport reactions involved the two databases for transport proteins, the TCDB (Saier et al., 2016) and the Transport Database (TransportDB) (Elbourne et al., 2017), and two computational tools, PSORTb v3.0 (Yu et al., 2010) and BLASTp (Altschul et al., 1990). We employed the following semi-automatic way of inferring the putative function of transport proteins in *M. capsulatus* (Bath).

Using the protein sequences in AE017282.2_protein.faa (Ward et al., 2004), we determined the subcellular location of each protein using PSORTb v3.0. We filtered the results and focused only on proteins with a final score larger than 7.5, which the authors of PSORTb consider to be meaningful. We combined this list with the *M. capsulatus* (Bath) specific entries from the TransportDB, which allowed us to use the PSORT-scores as an additional measure of confidence. At this point, 242 putative transport proteins were identified. From this list we then selected all proteins which were predicted to transport metabolites and were already included in the model, which reduced the number to 133. Since for many of the entries, the exact mechanism of transport is unknown, we combined the previously selected transporters with the results from running BLAST against the TCDB. The *e*-value and bitscore from BLAST provided yet another measure to confidently assess the correctness of the automatic TransportDB predictions, and the Transporter Classification-Numbers (TC-numbers) allowed us to gather information on the mechanism of transport. This led to a list of 97 transport proteins with high confidence, which was filtered once more as follows.

We checked the general description for a given specific TC-number, and then considered the BLAST result to read about a given transporter in more detail, especially with regards to finding the specific substrates. When we were able to identify the corresponding transport reaction in the BiGG database, we incorporated only the simplest, smallest set of reactions. In cases of conflicts between our own BLAST results and the automatic TransportDB transporter annotation, we preferentially trusted the BLAST results. Thus we ultimately added 75 transporter-encoding genes connected via GPR to 56 distinct transport reactions.

Applied Constraints

To identify which mode of electron transfer is active in *M. capsulatus* (Bath), we fit the solutions of flux balance analysis using iMcBath to measured values (Leak and Dalton, 1986a). The authors had experimentally determined the O_2/CH_4 ratio and the growth yield of *M. capsulatus* (Bath) in several conditions. They varied the nitrogen source using KNO_3, NH_4CL, and both

simultaneously; the concentration of copper in the medium, which directly affects the activity of either sMMO or pMMO; and whether the culture was oxygen or carbon limited.

The baseline constraints applied to the model allowed only the uptake of CH_4, O_2, SO_4, PO_4, either NH_4 or NO_3, and an array of mineral salts which are required by the biomass equation. The methane uptake rate was limited to allow at most 18.46 mmol $g_{DW}{}^{-1}$ h^{-1} (adopted from de la Torre et al., 2015), all remaining uptake rates were left unconstrained. We accounted for the differential expression of ADH (model reaction ID: ALAD_L) in the presence of excess NH_4 in the medium by blocking the GS/GOGAT (model reaction ID: GLNS). In the presence of NO_3 or N_2 we allowed flux through both reactions (Murrell and Dalton, 1983). Maximization of flux through the biomass equation was set as the objective for parsimonious flux balance analysis with which all calculations were done.

Since each electron transfer mode, respectively, is represented by the flux through one specific reaction in the model (model reaction IDs: *redox-arm* = PMMOipp, *direct coupling* = PMMODCipp, and *uphill electron transfer* = CYOR_q8ppi), we were able to investigate each simply by allowing flux through the corresponding reaction.

Several studies have shown that NH_4 is a co-metabolic substrate to the methane monooxygenases in *M. capsulatus* (Bath) leading to the production of hydroxylamine first and nitrite later (Hutton and Zobell, 1953; Bédard and Knowles, 1989; Nyerges and Stein, 2009). Hence, when simulating the growth on NH_4 we assumed that varying ratios r of the nitrogen taken up would eventually be converted into nitrite (**Figure 7**).

$$v_{EX_{nh4e}} + r v_{EX_{no2e}} = 0 \tag{2}$$

The program code and data for all analyses presented in this publication are available as *Model 15 Calculations.ipynb* at https://github.com/ChristianLieven/memote-m-capsulatus.

Stoichiometric Modeling

The reactome of an organism can be represented mathematically as a stoichiometric matrix S. Each row of S corresponds to a unique compound, while each column corresponds to a metabolic reaction. Hence the structure of the matrix for an organism with m compounds and n reactions equals $m \times n$. The values in each row denote the stoichiometric coefficients of that metabolite in all reactions. The coefficients are either negative for compounds that are educts, positive for those that are products, or zero for those that are not involved in a given metabolic reaction.

The vector v of length n contains as values the turnover rates of each reaction. These rates are commonly referred to as fluxes and are given the unit mmol gDW^{-1} h^{-1}. Vector v is also referred to as the flux vector.

AVAILABILITY OF DATA AND MATERIALS

The metabolic model, scripts and corresponding datasets generated and/or analyzed during the current study are available in the GitHub repository.

1. Archived: https://github.com/ChristianLieven/memote-m-capsulatus
2. Most Recent: https://github.com/ChristianLieven/memote-m-capsulatus/tree/develop

The data that support the biomass equation constructed in this study are available from Unibio at

1. http://www.unibio.dk/end-product/chemical-composition-1
2. http://www.unibio.dk/end-product/chemical-composition-2

Restrictions may apply to the accessibility of these data. Data are however available from the authors upon reasonable request and with permission of Unibio.

AUTHOR CONTRIBUTIONS

CL collected and analyzed the data, reconstructed the metabolic model, drafted and revised the manuscript. LP and SJ provided feedback on the metabolic behavior of *M. capsulatus* (Bath), discussed improvements to the model and revised the manuscript. KG, MH, and NS conceived and supervised the study and revised the manuscript critically. All authors read and approved the manuscript.

FUNDING

This work has been funded by the Novo Nordisk Foundation and the Innovation Fund Denmark [project "Environmentally Friendly Protein Production (EFPro2)"].

ACKNOWLEDGMENTS

The authors would like to acknowledge Budi Juliman Hidayat, Subir Kumar Nandi, and John Villadsen for sharing their experiences with *M. capsulatus* (Bath), Mitch Pesesky, David Collins, Marina Kalyuzhnaya, Ilya Akberdin, and Sergey Stolyar for insightful discussions at the GRC C1 Conference 2016, and Kristian Jensen, Joao Cardoso, and Marta Matos for their help with software problems and feedback on the implementation.

SUPPLEMENTARY MATERIAL

The Supplementary Material for this article can be found online at: https://www.frontiersin.org/articles/10.3389/fmicb.2018.02947/full#supplementary-material

FIGURE S1 | Genome-scale Metabolic Map. High-resolution image of the genome-scale metabolic map of iMcBath. The metabolic map was constructed using escher.

TABLE S1 | Stoichiometry of the biomass reaction in iMcBath. Table showing the stoichiometry and references of all components in the biomass reaction.

TABLE S2 | iMcBath performance overview. Predicted uptake rates, growth rates, growth yield and performance ratios in various conditions. The script that generated this table is available online in the corresponding GitHub repository: https://github.com/ChristianLieven/memote-m-capsulatus.

REFERENCES

Adeosun, E. K., Smith, T. J., Hoberg, A. M., Velarde, G., Ford, R., and Dalton, H. (2004). Formaldehyde dehydrogenase preparations from *Methylococcus capsulatus* (Bath) comprise methanol dehydrogenase and methylene tetrahydromethanopterin dehydrogenase. *Microbiology* 150, 707–713. doi: 10.1099/mic.0.26707-0

Altschul, S. F., Gish, W., Miller, W., Myers, E. W., and Lipman, D. J. (1990). Basic local alignment search tool. *J. Mol. Biol.* 215, 403–410. doi: 10.1016/S0022-2836(05)80360-2

Anthony, C. (1978). The prediction of growth yields in methylotrophs. *Microbiology* 104, 91–104.

Anthony, C. (1983). *The Biochemistry of Methylotrophs*. London: Academic Press. doi: 10.1016/0300-9629(83)90116-0

Anthony, C. (1992). The c-type cytochromes of methylotrophic bacteria. *Biochim. Biophys. Acta* 1099, 1–15. doi: 10.1016/0005-2728(92)90181-Z

Baxter, N. J., Hirt, R. P., Bodrossy, L., Kovacs, K. L., Embley, T. M., Prosser, J. I., et al. (2002). The ribulose-1,5-bisphosphate carboxylase/oxygenase gene cluster of *Methylococcus capsulatus* (Bath). *Arch. Microbiol.* 177, 279–289. doi: 10.1007/s00203-001-0387-x

Bédard, C., and Knowles, R. (1989). Physiology, biochemistry, and specific inhibitors of CH4, $NH4^+$, and CO oxidation by methanotrophs and nitrifiers. *Microbiol. Rev.* 53, 68–84.

Benedict, M. N., Gonnerman, M. C., Metcalf, W. W., and Price, N. D. (2012). Genome-scale metabolic reconstruction and hypothesis testing in the methanogenic archaeon *Methanosarcina acetivorans* C2A. *J. Bacteriol.* 194, 855–865. doi: 10.1128/JB.06040-11

Bergmann, D. J., Zahn, J. A., Hooper, A. B., and DiSpirito, A. A. (1998). Cytochrome P460 genes from the methanotroph *Methylococcus capsulatus* bath. *J. Bacteriol.* 180, 6440–6445.

Bernard, T., Bridge, A., Morgat, A., Moretti, S., Xenarios, I., and Pagni, M. (2014). Reconciliation of metabolites and biochemical reactions for metabolic networks. *Brief. Bioinform.* 15, 123–135. doi: 10.1093/bib/bbs058

Bird, C. W., Lynch, J. M., Pirt, F. J., Reid, W. W., Brooks, C. J. W., and Middleditch, B. S. (1971). Steroids and Squalene in *Methylococcus capsulatus* grown on Methane. *Nature* 230, 473–474. doi: 10.1038/230473a0

Blazyk, J. L., and Lippard, S. J. (2002). Expression and characterization of ferredoxin and flavin adenine dinucleotide binding domains of the reductase component of soluble methane monooxygenase from *Methylococcus capsulatus* (Bath). *Biochemistry* 41, 15780–15794. doi: 10.1021/bi026757f

Büchel, F., Rodriguez, N., Swainston, N., Wrzodek, C., Czauderna, T., Keller, R., et al. (2013). Path2Models: large-scale generation of computational models from biochemical pathway maps. *BMC Syst. Biol.* 7:116. doi: 10.1186/1752-0509-7-116

Campbell, M. A., Nyerges, G., Kozlowski, J. A., Poret-Peterson, A. T., Stein, L. Y., and Klotz, M. G. (2011). Model of the molecular basis for hydroxylamine oxidation and nitrous oxide production in methanotrophic bacteria. *FEMS Microbiol. Lett.* 322, 82–89. doi: 10.1111/j.1574-6968.2011.02340.x

Caspi, R., Altman, T., Billington, R., Dreher, K., Foerster, H., Fulcher, C. A., et al. (2014). The MetaCyc database of metabolic pathways and enzymes and the BioCyc collection of Pathway/Genome Databases. *Nucleic Acids Res.* 42, D459–D471. doi: 10.1093/nar/gkt1103

Chang, R. L., Ghamsari, L., Manichaikul, A., Hom, E. F. Y., Balaji, S., Fu, W., et al. (2011). Metabolic network reconstruction of Chlamydomonas offers insight into light-driven algal metabolism. *Mol. Syst. Biol.* 7:518. doi: 10.1038/msb.2011.52

Colby, J., and Dalton, H. (1978). Resolution of the methane mono-oxygenase of *Methylococcus capsulatus* (Bath) into three components. Purification and properties of component C, a flavoprotein. *Biochem. J.* 171, 461–468. doi: 10.1042/bj1710461

Colby, J., and Dalton, H. (1979). Characterization of the second prosthetic group of the flavoenzyme NADH–acceptor reductase (component C) of the methane mono-oxygenase from *Methylococcus capsulatus* (Bath). *Biochem. J.* 177, 903–908. doi: 10.1042/bj1770903

Culpepper, M. A., and Rosenzweig, A. C. (2014). Structure and protein–protein interactions of methanol dehydrogenase from *Methylococcus capsulatus* (Bath). *Biochemistry* 53, 6211–6219. doi: 10.1021/bi500850j

Dawson, M. J., and Jones, C. W. (1981). Energy conservation in the terminal region of the respiratory chain of the methylotrophic bacterium *Methylophilus methylotrophus*. *Eur. J. Biochem.* 118, 113–118. doi: 10.1111/j.1432-1033.1981.tb05492.x

de la Torre, A., Metivier, A., Chu, F., Laurens, L. M., Beck, D. A., Pienkos, P. T., et al. (2015). Genome-scale metabolic reconstructions and theoretical investigation of methane conversion in *Methylomicrobium buryatense* strain 5G(B1). *Microb. Cell Fact.* 14:188. doi: 10.1186/s12934-015-0377-3

DiSpirito, A. A., Kunz, R. C., Choi, D.-W., and Zahn, J. A. (2004). "Respiration in methanotrophs," in *Respiration in archaea and bacteria*, ed. D. Zannoni (Berlin: Springer), 149–168. doi: 10.1007/978-1-4020-3163-2_7

Ebrahim, A., Lerman, J. A., Palsson, B. O., and Hyduke, D. R. (2013). COBRApy: cOnstraints-based reconstruction and analysis for python. *BMC Syst. Biol.* 7:74. doi: 10.1186/1752-0509-7-74

Elbourne, L. D. H., Tetu, S. G., Hassan, K. A., and Paulsen, I. T. (2017). TransportDB 2.0: a database for exploring membrane transporters in sequenced genomes from all domains of life. *Nucleic Acids Res.* 45, D320–D324. doi: 10.1093/nar/gkw1068

Feist, A. M., Nagarajan, H., Rotaru, A.-E. E., Tremblay, P.-L. L., Zhang, T., Nevin, K. P., et al. (2014). Constraint-based modeling of carbon fixation and the energetics of electron transfer in Geobacter metallireducens. *PLoS Comput. Biol.* 10:e1003575. doi: 10.1371/journal.pcbi.1003575

Feist, A. M., Zielinski, D. C., Orth, J. D., Schellenberger, J., Herrgard, M. J., and Palsson, B. O. (2010). Model-driven evaluation of the production potential for growth-coupled products of *Escherichia coli*. *Metab. Eng.* 12, 173–186. doi: 10.1016/j.ymben.2009.10.003

Foster, J. W., and Davis, R. H. (1966). A methane-dependent coccus, with notes on classification and nomenclature of obligate, methane-utilizing bacteria. *J. Bacteriol.* 91, 1924–1931.

Ganter, M., Bernard, T., Moretti, S., Stelling, J., and Pagni, M. (2013). MetaNetX.org: a website and repository for accessing, analysing and manipulating metabolic networks. *Bioinformatics* 29, 815–816. doi: 10.1093/bioinformatics/btt036

Hanson, R. S., and Hanson, T. E. (1996). Methanotrophic bacteria. *Microbiol. Rev.* 60, 439–471.

Harder, W., and Van Dijken, J. P. (1976). "Theoretical considerations on the relation between energy production and growth of methane-utilizing bacteria," in *Microbial Production and Utilization of Gases,* eds H. G. Schlegel, N. Pfennig and G. Gottschalk (Gottingen: Goltze Verlag), 403–418.

Hommes, N. G., Sayavedra-Soto, L. A., and Arp, D. J. (2003). Chemolithoorganotrophic growth of Nitrosomonas europaea on fructose. *J. Bacteriol.* 185, 6809–6814. doi: 10.1128/JB.185.23.6809-6814.2003

Hutton, W. E., and Zobell, C. E. (1953). Production of nitrite from ammonia by methane oxidizing bacteria. *J. Bacteriol.* 65, 216–219.

Indrelid, S., Kleiveland, C., Holst, R., Jacobsen, M., and Lea, T. (2017). The soil bacterium *Methylococcus capsulatus* bath interacts with human dendritic cells to modulate immune function. *Front. Microbiol.* 8:320. doi: 10.3389/fmicb.2017.00320

Jiang, H., Chen, Y., Jiang, P., Zhang, C., Smith, T. J., Murrell, J. C., et al. (2010). Methanotrophs: multifunctional bacteria with promising applications in environmental bioengineering. *Biochem. Eng. J.* 49, 277–288. doi: 10.1016/j.bej.2010.01.003

Joergensen, L., and Degn, H. (1987). Growth rate and methane affinity of a turbidostatic and oxystatic continuous culture of *Methylococcus Capsulatus* (BATH). *Biotechnol. Lett.* 9, 71–76. doi: 10.1007/BF01043398

Kalyuzhnaya, M. G. (2016). "Methane biocatalysis: selecting the right microbe," in *Biotechnology for Biofuel Production and Optimization*, eds C. Eckert and C. Trinh (Amsterdam: Elsevier B.V). doi: 10.1016/B978-0-444-63475-7.00013-3

Kelly, D. P., Anthony, C., and Murrel, J. C. (2005). Insights into the obligate methanotroph *Methylococcus capsulatus*. *Trends Microbiol.* 13, 195–198. doi: 10.1016/j.tim.2005.03.002

Kim, B., Kim, W. J., Kim, D. I., and Lee, S. Y. (2015). Applications of genome-scale metabolic network model in metabolic engineering. *J. Ind. Microbiol. Biotechnol.* 42, 339–348. doi: 10.1007/s10295-014-1554-9

King, Z. A., Dräger, A., Ebrahim, A., Sonnenschein, N., Lewis, N. E., and Palsson, B. O. (2015). Escher: a web application for building, sharing, and embedding data-rich visualizations of biological pathways. *PLoS Comput. Biol.* 11:e1004321. doi: 10.1371/journal.pcbi.1004321

King, Z. A., Lu, J., Dräger, A., Miller, P., Federowicz, S., Lerman, J. A., et al. (2016). BiGG Models: a platform for integrating, standardizing and sharing genome-scale models. *Nucleic Acids Res.* 44, D515–D522. doi: 10.1093/nar/gkv1049

Kleiveland, C. R., Hult, L. T. O., Spetalen, S., Kaldhusdal, M., Christofferesen, T. E., Bengtsson, O., et al. (2013). The noncommensal bacterium *Methylococcus capsulatus* (Bath) ameliorates dextran sulfate (sodium salt)-induced ulcerative colitis by influencing mechanisms essential for maintenance of the colonic barrier function. *Appl. Environ. Microbiol.* 79, 48–57. doi: 10.1128/AEM.02464-12

Larsen, Ø., and Karlsen, O. A. (2016). Transcriptomic profiling of *Methylococcus capsulatus* (Bath) during growth with two different methane monooxygenases. *Microbiologyopen* 5, 254–267. doi: 10.1002/mbo3.324

Leak, D. J., and Dalton, H. (1983). In vivo studies of primary alcohols, aldehydes and carboxylic acids as electron donors for the methane mono-oxygenase in a variety of methanotrophs. *Microbiology* 129, 3487–3497. doi: 10.1099/00221287-129-11-3487

Leak, D. J., and Dalton, H. (1986a). Growth yields of methanotrophs - 1. Effect of copper on the energetics of methane oxidation. *Appl. Microbiol. Biotechnol.* 23, 470–476. doi: 10.1007/BF02346062

Leak, D. J., and Dalton, H. (1986b). Growth yields of methanotrophs 2. A theoretical analysis. *Appl. Microbiol. Biotechnol.* 23, 477–481. doi: 10.1007/BF02346063

Lund, J., Woodland, M. P., and Dalton, H. (1985). Electron transfer reactions in the soluble methane monooxygenase of *Methylococcus capsulatus* (Bath). *Eur. J. Biochem*. 147, 297–305. doi: 10.1111/j.1432-1033.1985.tb08750.x

Makula, R. A. (1978). Phospholipid composition of methane-utilizing bacteria. *J. Bacteriol.* 134, 771–777.

Mishra, N. K., Chang, J., and Zhao, P. X. (2014). Prediction of membrane transport proteins and their substrate specificities using primary sequence information. *PLoS One* 9:e100278. doi: 10.1371/journal.pone.0100278

Moretti, S., Martin, O., Van Du Tran, T., Bridge, A., Morgat, A., and Pagni, M. (2016). MetaNetX/MNXref–reconciliation of metabolites and biochemical reactions to bring together genome-scale metabolic networks. *Nucleic Acids Res.* 44, D523–D526. doi: 10.1093/nar/gkv1117

Müller, H., Hellgren, L. I., Olsen, E., and Skrede, A. (2004). Lipids rich in phosphatidylethanolamine from natural gas-utilizing bacteria reduce plasma cholesterol and classes of phospholipids: a comparison with soybean oil. *Lipids* 39, 833–841. doi: 10.1007/s11745-004-1304-15

Murrell, J. C., and Dalton, H. (1983). Ammonia assimilation in *Methylococcus capsulatus* (Bath) and other obligate methanotrophs. *J. Gen. Microbiol.* 129, 1197–1206. doi: 10.1099/00221287-129-4-1197

Murrell, J. C., Dalton, H., Murrell, J., Colin, Dalton, H., Colin Murrell, J., Dalton, H., et al. (1983). Nitrogen fixation in obligate methanotrophs. *Microbiology* 129, 3481–3486. doi: 10.1099/00221287-129-11-3481

Myronova, N., Kitmitto, A., Collins, R. F., Miyaji, A., and Dalton, H. (2006). Three-dimensional structure determination of a protein supercomplex that oxidizes methane to formaldehyde in *Methylococcus capsulatus* (Bath). *Biochemistry* 45, 11905–11914. doi: 10.1021/bi061294p

Nagarajan, H., Sahin, M., Nogales, J., Latif, H., Lovley, D. R., Ebrahim, A., et al. (2013). Characterizing acetogenic metabolism using a genome-scale metabolic reconstruction of *Clostridium ljungdahlii*. *Microb. Cell Fact.* 12:118. doi: 10.1186/1475-2859-12-118

Nakano, C., Motegi, A., Sato, T., Onodera, M., and Hoshino, T. (2007). Sterol biosynthesis by a prokaryote: first in vitro identification of the genes encoding squalene epoxidase and lanosterol synthase from *Methylococcus capsulatus*. *Biosci. Biotechnol. Biochem.* 71, 2543–2550. doi: 10.1271/bbb.70331

Neidhardt, F. C., Ingraham, J. L., and Schaechter, M. (1990). *Physiology of the Bacterial Cell: a Molecular Approach*. Sunderland, MA: Sinauer Associates.

Nogales, J., Gudmundsson, S., Knight, E. M., Palsson, B. O., and Thiele, I. (2012). Detailing the optimality of photosynthesis in cyanobacteria through systems biology analysis. *Proc. Natl. Acad. Sci. U.S.A.* 109, 2678–2683. doi: 10.1073/pnas.1117907109

Nunes, J. J., Aufderheide, B., Ramjattan, D. M., and Dass, R. (2016). Enhanced production of single cell protein from *M. capsulatus* (Bath) growing in mixed culture. *J. Microbiol. Biotechnol. Food Sci.* 6, 894–899. doi: 10.15414/jmbfs.2016/17.6.3.894-899

Nyerges, G., and Stein, L. Y. (2009). Ammonia cometabolism and product inhibition vary considerably among species of methanotrophic bacteria. *FEMS Microbiol. Lett.* 297, 131–136. doi: 10.1111/j.1574-6968.2009.01674.x

Oakley, C. J., and Murrell, J. C. (1991). Cloning of nitrogenase structural genes from the obligate methanotroph *Methylococcus capsulatus* (Bath). *FEMS Microbiol. Lett*. 62, 121–125. doi: 10.1111/j.1574-6968.1991.tb04429.x

Olivier, B. G., and Bergmann, F. T. (2015). The systems biology markup language (SBML) level 3 package: flux balance constraints. *J. Integr. Bioinform.* 12:269. doi: 10.2390/biecoll-jib-2015-269

Orth, J. D., Conrad, T. M., Na, J., Lerman, J. A., Nam, H., Feist, A. M., et al. (2011). A comprehensive genome-scale reconstruction of *Escherichia coli* metabolism–2011. *Mol. Syst. Biol.* 7:535. doi: 10.1038/msb.2011.65

Øverland, M., Tauson, A.-H., Shearer, K., and Skrede, A. (2010). Evaluation of methane-utilising bacteria products as feed ingredients for monogastric animals. *Arch. Anim. Nutr.* 64, 171–189. doi: 10.1080/17450391003691534

Patel, R. N., and Hoare, D. S. (1971). Oxidation of C-1 compounds capsulatus physiological studies of methane and methanol- oxidizing bacteria?: oxidation of c-1 compounds by *Methylococcus capsulatus*. *J. Bacteriol.* 107, 187–192.

Petersen, L. A. H., Villadsen, J., Jørgensen, S. B., and Gernaey, K. V. (2017). Mixing and mass transfer in a pilot scale U-loop bioreactor. *Biotechnol. Bioeng.* 114, 344–354. doi: 10.1002/bit.26084

Reshetnikov, A. S., Rozova, O. N., Khmelenina, V. N., Mustakhimov, I. I., Beschastny, A. P., Murrell, J. C., et al. (2008). Characterization of the pyrophosphate-dependent 6-phosphofructokinase from *Methylococcus capsulatus* Bath. *FEMS Microbiol. Lett.* 288, 202–210. doi: 10.1111/j.1574-6968.2008.01366.x

Ritala, A., Häkkinen, S. T., Toivari, M., and Wiebe, M. G. (2017). Single cell protein—state-of-the-art, industrial landscape and patents 2001–2016. *Front. Microbiol.* 8:2009. doi: 10.3389/fmicb.2017.02009

Ross, M. O., and Rosenzweig, A. C. (2017). A tale of two methane monooxygenases. *J. Biol. Inorg. Chem.* 22, 307–319. doi: 10.1007/s00775-016-1419-y

Rozova, O. N., Khmelenina, V. N., Mustakhimov, I. I., Reshetnikov, A. S., and Trotsenko, Y. A. (2010). Characterization of recombinant fructose 1, 6 bisphosphate aldolase from *Methylococcus capsulatus* bath. *Biochemistry* 75, 892–898.

Saier, M. H. Jr., Tran, C. V., and Barabote, R. D. (2006). TCDB: the Transporter Classification Database for membrane transport protein analyses and information. *Nucleic Acids Res.* 34, D181–D186. doi: 10.1093/nar/gkj001

Saier, M. H., Reddy, V. S., Tsu, B. V., Ahmed, M. S., Li, C., and Moreno-Hagelsieb, G. (2016). The Transporter Classification Database (TCDB): recent advances. *Nucleic Acids Res.* 44, D372–D379. doi: 10.1093/nar/gkv1103

Shiemke, A. K., Arp, D. J., and Sayavedra-Soto, L. A. (2004). Inhibition of membrane-bound methane monooxygenase and ammonia monooxygenase by diphenyliodonium: implications for electron transfer. *J. Bacteriol.* 186, 928–937. doi: 10.1128/JB.186.4.928-937.2004

Stanley, S. H., and Dalton, H. (1982). Role of Ribulose-l, 5-bisphosphate Carboxylase / Oxygenase in. *J. Gen. Microbiol.* 128, 2927–2935.

Strøm, T., Ferenci, T., and Quayle, J. R. (1974). The carbon assimilation pathways of *Methylococcus capsulatus*, *Pseudomonas methanica* and *Methylosinus trichosporium* (OB3B) during growth on methane. *Biochem. J.* 144, 465–476. doi: 10.1042/bj1440465

Tate, S., and Dalton, H. (1999). A low-molecular-mass protein from *Methylococcus capsulatus* (Bath) is responsible for the regulation of formaldehyde dehydrogenase activity in vitro. *Microbiology* 145(Pt 1), 159–167. doi: 10.1099/13500872-145-1-159

Taylor, S. (1977). Evidence for the presence of ribulose 1,5-bisphosphate carboxylase and phosphoribonuclease in *Methylococcus capsulatus* (bath). *FEMS Microbiol. Lett.* 2, 305–307. doi: 10.1016/0378-1097(77)90057-x

Taylor, S., Dalton, H., and Dow, C. (1980). Purification and initial characterisation of ribulose 1,5-bisphosphate carboxylase from *Methylococcus capsulatus* (Bath). *FEMS Microbiol. Lett.* 8, 157–160. doi: 10.1016/0378-1097(80)90021-x

Taylor, S. C., Dalton, H., and Dow, C. S. (1981). Ribulose- 1,5-bisphosphate carboxylase/oxygenase and carbon assimilation in *Methylococcus capsulatus* (Bath). *Microbiology* 122, 89–94. doi: 10.1099/00221287-122-1-89

Thiele, I., and Palsson, B. Ø. (2010). A protocol for generating a high-quality genome-scale metabolic reconstruction. *Nat. Protoc.* 5, 93–121. doi: 10.1038/nprot.2009.203

Unibio (2018). *Unibio Homepage*. Available at: www.unibio.dk

Varma, A., Boesch, B. W., and Palsson, B. O. (1993). Stoichiometric interpretation of *Escherichia coli* glucose catabolism under various oxygenation rates. *Appl. Environ. Microbiol.* 59, 2465–2473.

Vorholt, J. A. (2002). Cofactor-dependent pathways of formaldehyde oxidation in methylotrophic bacteria. *Arch. Microbiol.* 178, 239–249. doi: 10.1007/s00203-002-0450-2

Ward, N., Larsen, Ø., Sakwa, J., Bruseth, L., Khouri, H., Durkin, A. S., et al. (2004). Genomic insights into methanotrophy: the complete genome sequence of *Methylococcus capsulatus* (Bath). *PLoS Biol.* 2:e303. doi: 10.1371/journal.pbio.0020303

Wolfe, R. S., and Higgins, I. J. (1979). Microbial biochemistry of methane-a study in contrasts. *Int. Rev. Biochem.* 21, 267–353.

Wood, A. P., Aurikko, J. P., and Kelly, D. P. (2004). A challenge for 21st century molecular biology and biochemistry: what are the causes of obligate autotrophy and methanotrophy? *FEMS Microbiol. Rev.* 28, 335–352. doi: 10.1016/j.femsre.2003.12.001

Yu, N. Y., Wagner, J. R., Laird, M. R., Melli, G., Rey, S., Lo, R., et al. (2010). PSORTb 3.0: improved protein subcellular localization prediction with refined localization subcategories and predictive capabilities for all prokaryotes. *Bioinformatics* 26, 1608–1615. doi: 10.1093/bioinformatics/btq249

Zahn, J. A., Bergmann, D. J., Boyd, J. M., Kunz, R. C., and DiSpirito, A. A. (2001). Membrane-associated quinoprotein formaldehyde dehydrogenase from *Methylococcus capsulatus* Bath. *J. Bacteriol.* 183, 6832–6840. doi: 10.1128/JB.183.23.6832-6840.2001

Conflict of Interest Statement: Unibio is a collaborator in the "Environmentally Friendly Protein Production (EFPro2)" project. CL, MH, and NS are publicly funded through the Novo Nordisk Foundation and the Innovation Fund Denmark.

The remaining authors declare that the research was conducted in the absence of any commercial or financial relationships that could be construed as a potential conflict of interest.

Copyright © 2018 Lieven, Petersen, Jørgensen, Gernaey, Herrgard and Sonnenschein. This is an open-access article distributed under the terms of the Creative Commons Attribution License (CC BY). The use, distribution or reproduction in other forums is permitted, provided the original author(s) and the copyright owner(s) are credited and that the original publication in this journal is cited, in accordance with accepted academic practice. No use, distribution or reproduction is permitted which does not comply with these terms.